

Failure analysis of timber bolted joints by fracture mechanics

L. DAUDEVILLE

*Laboratoire de Mécanique et Technologie, ENS / CNRS / Univ. Paris 6
61 avenue du Président Wilson, 94230 CACHAN CEDEX, FRANCE
also at IUT de Marne-La-Vallée*

M. YASUMURA

Building Research Institute, 1-Tatehara, TSUKUBA, 305 JAPAN

This study concerns the failure of dowel-type joints in glued laminated timber under static loading. Failure of joints with a single bolt or dowel due to cracking parallel to the grain direction is considered. Presented results concern only the first mode of cracking i.e. splitting under tension perpendicular to grain. Fracture is analyzed by use of linear elastic fracture mechanics concepts (LEFM), the crack propagation condition is assumed to be based upon the critical energy release rate G_{Ic} . A simplified average stress criterion allows the prediction of the splitting onset.

An experimental program was carried out on joints for different structural parameters and bolt diameters. The experimental stable crack growth allowed to obtain the load-crack length curves. An other experimental program was carried out in order to compare the fracture energy of a few CIB-type specimens with the critical energy release rate G_{Ic} used in the crack propagation simulation.

The comparison between experimental and numerical results for the simulation of fracture in joints shows that LEFM provides a good approximation of load-bearing capacity of bolted joints and may help improve design codes.

1. INTRODUCTION

Engineering methods for the design of timber mechanical joints are based upon Johansen's yield model [1] [2] [3] [4] [5]. This limit analysis method includes connector limit states but does not take into account the various modes of degradation of wood: cracking parallel to the grain under tearing (mode I) or shearing (mode II and III), failure under tension along the grain direction. Some damage mechanisms are brittle others are more progressive. Concerning the timber, only the crushing at the bolt and wood contact is considered in the Johansen limit analysis.

Normally, bolted joints are designed with the intent of avoiding brittle failure modes associated with catastrophic crack growth parallel to the grain. Nevertheless the study of that failure mode is necessary to incorporate in the international codes a reliable method of design of mechanical joints.

Eurocode 5 [2] proposition for the verification of resistance to a solicitation which is not along the grain direction consists into the comparison of a mean shear stress with a critical value. That criterion may not be convenient because it does not take into account the failure mode and the possible existence of a crack.

The aim of this study is the prediction of failure of joints with a single bolt or dowel under a static loading perpendicular to the grain (see Fig. 1). The structural parameters are the bolt diameter d , the end-distance e_1 and the edge-distance e_2 . In that particular case, the failure mode is known. A crack appears at the end of the bolt hole and propagates parallel to the grain (L direction) along the weakest plane of wood. This failure mechanism is generally brittle but the ratio of initiation and ultimate loads can be about 55% for large values of e_1 and e_2 . Thus failure analysis can be applied separately into the study of the initiation of a crack and into that of the propagation of an existing crack.

Numerous and experimental studies of mechanical bolted joints have been conducted [6] [7] [8]. Rahman et al. [7] combine a finite element analysis with orthotropic criteria to predict initial joint failure when the load is applied parallel to grain. Previous study and [8] take into account the non-linear stress-strain behavior of the wood and the friction between the wood and the bolt. These studies are very interesting to investigate the influences of bolt-spacing, end-

distance and edge-distance of a multiple fastener when bolts load members parallel to grain because in that particular case non-linear phenomena have a major influence on stress distribution. The crack propagation was not investigated in previous studies.

For the studied problem i.e. a perpendicular to the grain loading, wood is assumed to respond linear-elastically to failure. Whitney and Nuismer [9] proposed for composite materials a simplified stress fracture criterion based on the actual stress distribution near a hole or a notch. Following this approach, the initiation of a crack is assumed to occur when the average elastic stress perpendicular to grain over a characteristic distance from the boundary of the hole equals the tensile strength of the material with no hole. A further investigation is necessary to know if the characteristic distance (or volume) is unique or not for different fracture modes and if it can be linked to the structure of wood for given species.

Crack propagation is analyzed by use of classical linear elastic fracture mechanics (LEFM). Application of fracture mechanics to wood has principally concerned the analysis of test specimens for the evaluation of fracture properties [10] [11] [12]. For the analysis of mechanical joints fracture mechanics methods have been scarcely applied. Non linear phenomena that occur in the so-called process zone of non linear fracture mechanics are not considered [13]. In other words it means that the size of the process zone is neglected in mechanical joints. We combined LEFM with a Griffith criterion based upon the critical energy release rate G_c . The energy release rate is computed with respect to the crack length by the compliance method. Both initiation and propagation were studied with the finite element (FE) code CASTEM 2000.

Failure tests of joints were carried out for different bolt diameters, edge-distances and end-distances. The wood member was composed of glued laminated spruce. The initiation load, the crack length with respect to the load were noted. The only parameter of the modeling that has been identified with these tests is the critical energy release rate G_{Ic} . In order to verify the validity of the experimentally identified critical energy release rate G_{Ic} , that is characteristic of wood species, a few CIB-type specimens were tested to determine the fracture energy G_{If} according to the Draft Standard [10]. Comparisons between experimental and numerical results for studied single bolted joints with a perpendicular to the grain

loading are presented. Initiation and ultimate loads and also the load with respect to the crack length are given.

2. EXPERIMENTAL STUDY OF MECHANICAL JOINTS

Mechanical joints have been tested at the Laboratory of Mechanics and Technology (LMT) of Cachan [14]. The moisture content and the density of glued laminated members were 10% and 0.46. Wood species is spruce. The fasteners are not bolts but steel shafts in order to create a "perfect" contact i.e. with no allowance between the wood and the shaft.

d is the shaft diameter, b is the wood member thickness, e_1 and e_2 are respectively the end- and edge-distances (see Fig. 1). Table 1 presents the different kinds of specimens. For each kind, only a few tests (from 2 to 5) have been performed. Contrary to the case of a parallel to the grain loading, the member thickness b has not a major influence because the bending of the bolt is negligible.

Classical strain gages were used on one face, crack detection (CD) gages on the other one (see CD gages on Fig. 2).

Specimens were tested to failure in stroke displacement control with a head speed of 2.25×10^{-2} mm/min. This low speed is chosen in order to detect the initiation and to follow easily the stable crack propagation. Rather than the stroke displacement, the displacement between the steel plates and wooden member was measured with electronic transducers. Load, strain and displacement were recorded by a HP workstation at a rate of 1 Hz.

The A1-4 and A1-5 specimens (see Table 1 & 2) were tested with a speed of 0.18 mm/min to fail in about 300 s as recommended in Eurocode 5 [2]. We did not notice any important effects on the maximum load of these specimens.

The initiation was detected by considering the three following criteria:

- (i) a CD gage near the hole is cut
- (ii) a drop in load is observed
- (iii) a cracking is heard

(ii) criterion is suggested by the fact that a cracking will decrease the specimen stiffness. When this decrease is a result of instantaneous splitting in a joint which is

quasi-statically loaded under stroke control, the result is an instantaneous drop in load (which may be very small).

Two of the three above criteria had to be verified to consider that initiation occurred (generally (ii) and (iii)). Table 2 gives the initiation and ultimate loads (the ultimate load is the maximum load).

Fig. 3 and Fig. 4 are respectively the load-displacement curves for the B2-4 (d=20 mm) and C1-1 (d=12 mm) specimens. Fig. 5 curve corresponds to the load with respect to the strain in wood at the bolt and wood contact for the B2-4 specimen. Note an important non linearity due to crushing. This non linearity can also be observed on the load-displacement curves but after initiation non linear phenomena seem to be essentially due to splitting (according to the visual observation). Also note the important drop in load for the C1-1 specimen (Fig. 4) due to the presence of a knot.

3. MODELING AND SIMULATION

3.1. Assumptions

The modeling assumptions are:

H1 : Plane stress state

H2 : Wood is linear-elastic to failure

H3 : The bolt is a rigid body

H4 : The wood and bolt contact is perfect i.e. with no friction and no allowance

H5 : The transverse T and radial directions R are not distinguished i.e. the wood is transversally isotropic

The structure is modeled by finite elements. Because of symmetries, 1/2 of structure is studied (see Fig. 6).

H2 assumption relies on the observation of stress-strain responses that are quasi-linear until failure in tension and non-linear in compression [15].

For a plane problem, the radial R and transverse T directions (according to Johnson's notations [16]) cannot be distinguished so we considered a mean behavior. The elastic moduli were chosen by extrapolation of results [17] with respect to the actual density. x direction corresponds to the L direction (Fig. 6).

$$\begin{cases} E_x = 15000\text{MPa} , E_y = \frac{E_T + E_R}{2} = 600\text{MPa} \\ G_{xy} = \frac{G_{RL} + G_{TL}}{2} = 700\text{MPa} , \nu_{xy} = 0.5 \end{cases}$$

3.2. Initiation

The stress state is mainly a tensile one around the point B (see Fig. 6) while a compressive stress state is concentrated at the upper part of the bolt. Degradation takes place in these two regions. The initiation of cracking occurs at the point B (Fig. 6) where a high stress gradient exists. Different fracture criteria for wood exist in the literature [18]. They are expressed in terms of stresses in a co-ordinate system coinciding with the directions of orthotropy. The failure mode is a pure mode I then these criteria are reduced into the comparison of the tearing stress σ_{yy} with the tensile strength f_t for the cracking onset detection. The mean tensile strength for spruce species is (obtained by means of tensile tests performed at CTBA Paris [18]):

$$f_t = 4.76 \text{ MPa}$$

The computation of the local elastic stress $\sigma_{yy}(P_c)$ for the experimental initiation load P_c gives a stress value at the point B much higher than f_t . Note that in the case of a sharp crack the stress value is infinite. The application of a local approach seems difficult in the case of high stress gradients. In add, the mesh refinement needs to be very rich for a good approximation of local elastic stresses in the vicinity of the hole.

Whitney and Nuismer [9] proposed for composite materials a simplified stress fracture criterion based on the comparison of the average stress over a characteristic distance a_c with the tensile strength f_t . We applied this approach for the initiation detection. The criterion is (Fig. 7):

$$\frac{1}{a_c} \int_0^{a_c} \sigma_{yy}(P_c) dx = f_t$$

This "non local" criterion is less sensitive to the mesh refinement than the local one.

An other approach consists in the application of LEFM concepts for the initiation problem by assuming a pre-existing sharp crack. This approach was applied to wood by Sobue [20]. The length of the initial defect is assumed to be intrinsic. The concept of the latter criterion seems similar to that of the average stress criterion but the computation of the energy release rate or the stress intensity factor is difficult for a very short crack.

In order to identify the distance a_i , the stress distribution of each specimen denoted i is computed with the experimental initiation load $(P_c)_i$. This is a FE computation of the elastic stresses distribution. a_c is the mean value of the distances a_i for the n specimens.

$$a_c = \frac{1}{n} \sum_{i=1}^n a_i = 2.84 \text{ mm}$$

The important question is: Is a_c an intrinsic material parameter. It is difficult to answer "yes" categorically but we did not notice any large difference in the a_i values for the bolt diameters $d=12$ mm, 16 mm and 20 mm.

The experimental and simulation results concerning the initiation load are compared (see Fig. 8 and Fig. 9). These figures clearly show, in one hand the influence of the bolt diameter and, in another hand the quasi non influence of the edge-distance on the initiation load with an end-distance equal to $7d$. Table 3 gives the computed initiation load for each specimen to be compared with the experimental one in table 2.

A further investigation is necessary to know if the characteristic distance (or volume) a_c is an intrinsic parameter for other geometry and loading.

3.3. Propagation

The existence of a crack at the point B is now assumed (see Fig. 6). The propagation analysis is carried out by use of classical LEFM i.e. all damage phenomena are assumed to occur at the crack tip.

The energy release rate is:

$$G = - \frac{1}{b} \frac{W}{A} = \text{Erreur !; } A)$$

with

$$\begin{cases} W: \text{Potential energy} \\ A: \text{Crack length} \\ k: \text{Mechanical joint stiffness} \\ b: \text{Specimen width} \end{cases}$$

A Griffith criterion [21] for the crack propagation condition is chosen:

- $G(P,A) < G_c$ No crack propagation
- $G(P,A) = G_c$ Possible crack propagation ($P=P_c$)

and

$$\begin{cases} \frac{\partial G}{\partial A}(A) = 0 : \text{unstable propagation} \\ \frac{\partial G}{\partial A}(A) < 0 : \text{stable propagation} \end{cases}$$

$G_c = G_{Ic}$ is the critical energy release rate for a mode I cracking. The crack is parallel to the grain direction. $G(A,P)$ is computed by the compliance method, the crack propagation is modeled by separating two connected lines. The mesh refinement at the crack tip is constant during the crack propagation.

Thus for two F.E. computations 1 and 2:

$$\frac{G}{P^2} = \frac{1}{2b} \frac{1}{\Delta A} \left(\frac{1}{k_2} - \frac{1}{k_1} \right)$$

with $\Delta A = A_2 - A_1$ and $\Delta A \ll A$

The previous relationship allows to calculate the force with respect to the crack length for a given critical energy release rate G_{Ic} or for a given force to identify G_{Ic} . Fig. 10 and Fig. 11 represent the computed value $Y = G \left(\frac{b}{P} \right)^2$ with respect to the crack length A/d for $e_1 = 7d, 25d$ and for different values of the edge-distance e_2 .

For a monotonously increasing loading and for a Griffith criterion $G = G_{Ic}$, the minimum of the curve $Y(A) = G \left(\frac{b}{P} \right)^2$ is the transition point between a stable and a unstable crack propagation (see Fig. 10 and Fig. 11).

Let us define A_c and P_{cM} such that:

$$\frac{\partial G}{\partial A}(A_c, P_{cM}) = 0 \quad (\text{or } \frac{\partial Y}{\partial A}(A_c, P_{cM}) = 0) \quad \text{and } G(A_c, P_{cM}) = G_{Ic}$$

The previous loading P_{cM} is the maximum loading that the mechanical joint can bear. A_c is the critical crack length. The previous curves show that there may be a stable crack propagation as the load increases. The critical crack length A_c is about one and half times of bolt diameter with $e_1 = 7d$ and about six times of bolt diameter with $e_1 = 25d$. These results confirm that the joint does not fail just after the initiation of the crack.

During the controlled stroke displacement test the ultimate load was reached and the load-displacement curve after the maximum load was also obtained. Table 2 gives the experimental ultimate loads.

It was chosen to identify the critical energy release rate G_c for that maximum loading. The knowledge of $(P_{cM})_i$ for each test i allows to compute $(G_{Ic})_i$.

For instance, let us examine the specimen C1-1 ($e_1 = 25d$; $e_2 = 4d$; $d = 12\text{mm}$):

$$\left. \begin{array}{l} (P_{cM})_{C1-1} = 6.27 \text{ kN (Table 2)} \\ (A_c)_{C1} = 2,4d \\ (G_{Ic} \left(\frac{b}{P_{cM}}\right)^2)_{C1} = 6,11 \text{ m/kN (see Fig. 11)} \end{array} \right\} (G_{Ic})_{C1-1} = 186 \text{ N/m}$$

G_{Ic} is the mean value of the different $(G_{Ic})_i$:

$$G_{Ic} = 197 \text{ N/m}$$

The following simulation results were obtained with $G_{Ic} = 197 \text{ N/m}$. Fig. 12 shows the comparison between the experimental and computational load-crack length curves for the C1-1 test and for the cracks located on the left and the right part of the bolt. Table 3 gives the computed ultimate load for each specimen to be compared with the experimental one in table 2.

Fig. 13 shows the comparison between the computational and experimental ultimate loads for $d = 12 \text{ mm}$. The lines and the points represent respectively the simulations and the tests. Fig. 14 shows the influence of the bolt diameter.

It was chosen to compare the energy release rate with a critical value for the analysis of propagation of cracking. The same approach was applied with the concept of stress intensity factor. The results are similar. The analysis of a possible multiple cracking (for instance with several bolts) is computationally cheaper by using stress intensity factors because, in such a case, it is necessary to do a FE computation for each energy release rate corresponding to a possible crack propagation.

4. EXPERIMENTAL IDENTIFICATION OF THE FRACTURE ENERGY

According to LEFM concepts [21], G_c is defined as follows: While a crack starts to grow, the part of the stored elastic energy that is consumed by the fracture process at the crack tip per unit of new separation area is the critical energy release rate G_{Ic} (mode I).

Hence G_{Ic} is experimentally identified with the maximum load F_M that the specimen can bear during a fracture test (see Fig. 15). A relation can be established between the critical stress intensity factor K_{Ic} and the critical energy release rate G_{Ic} [12].

The fracture energy G_{If} dissipated during complete crack propagation can also be defined by the integration of the complete load-displacement curve ($F-\delta$) of the specimen (see Fig. 15):

$$G_{If} = \frac{1}{A_{lig}} \int_0^{\delta} F d\delta$$

A_{lig} is the area of the uncracked ligament before loading.

If non linear phenomena due to damage or plasticity are present during crack propagation in a process zone at the crack tip, LEFM is no longer applicable. The consequence is that G_{If} and G_{Ic} are non equal. In such a case non linear fracture mechanics can be used [12] [13] or also LEFM by using an effective crack length [22]. G_{Ic} is the fracture energy in a linear elastic material with no process zone.

For the studied problem, i.e. the analysis of fracture in a mechanical joint, we assumed that the process zone size is small compared with the crack length and

the structure size. Hence the influence of the process zone is negligible and LEFM can be applied by assuming the fracture energy G_{Ic} is equal to G_{If} .

In order to verify the previous assumption, i.e. to verify the validity of LEFM by using the toughness G_{If} , a few mode I fracture tests (about 30) were carried out at the Centre Technique du Bois et de l'Ameublement (CTBA Paris). The reference test method chosen is the bending test according to the CIB-Draft Standard [10] (see Fig. 16).

Rather than carrying out tests, G_{If} could have been taken from the literature [23] for the wood member species. In such a case, the fracture energy G_{If} from [23] is very different from G_{Ic} that was identified with the mechanical joints tests (about 80% of difference with $G_{Ic} = 197$ N/m).

These experiments consisted into a preliminary test program for the determination of the fracture energy of French spruce, results are given in [24] and [14].

Specimens were tested in stroke displacement control. The main features of the tests were:

- The head speed has been chosen lower than that recommended in [12] in order to have a stable cracking
- The initial defect shape is a triangular (see Fig. 16)
- The initial crack length is $A_0 = 0.6h$ (the specimen section is a square, $h = 45$ mm)

According to the results, the mean experimental fracture energy of spruce in tension perpendicular to grain and for a density of 460 kg/m³ is:

$$G_{If} \simeq 180 \text{ N/m}$$

Note that G_{If} is not identified with the maximum load F_M but with the area of the load displacement curve (see Fig. 15).

This result must be considered with caution because the results showed too much scatter to be able to propose a fracture energy value with so few specimens. Nevertheless the values of G_{Ic} and G_{If} are close that could confirm the validity of LEFM for the failure analysis of mechanical bolted joints.

5. CONCLUSION

LEFM is a simplified approach consisting in the comparison of the energy release rate with a critical value. This method has been applied for the determination of the load bearing capacity of a mechanical joint with a single bolt. The fracture mode was the mode I of opening. The critical energy release rate was obtained by testing mechanical joints. This result is in a good agreement with the fracture energy value that we obtained with bending fracture tests. Adjust this simplified approach for design codes might provide an improvement for the determination of the ultimate load in the design of bolted or nailed joints. The ultimate load may be much higher than the initiation load of cracking for large values of the end- and edge-distances. So, the mechanical joint does not fail just after the onset of cracking. The initiation load is also an important data in the design of mechanical joints. The onset of cracking has been predicted by use of an average stress criterion.

ACKNOWLEDGEMENTS

The authors would like to thank F. Dubois and A. Bengougam who carried out the experiments in Master's courses of ENS Cachan, and F. Rouger and J.D. Lanvin of CTBA for providing the specimens and advice.

REFERENCES

- [1] Johansen, K.W., "Theory of Timber Connections", Inter. Assoc. of Bridge and Structural Engineering, Bern, Switzerland, Publ. 9 (1949) 249-262
- [2] "EUROCODE 5 - Design of Timber Structure", ENV 1995-1-1, CEN, Brussels (1993)
- [3] Yasumura, M., Murota, T. and Sakai, H., "Ultimate Properties of Bolted Joints in Glued-laminated Timber", CIB-W18A Meeting, paper 20-7-3 (1987)
- [4] Yasumura, M., "Japan Overview: Design Concept and Prospect of Bolted Joints and Nailed Joints", Proceedings of International Workshop on Wood Connectors, Ed. Forest Products Society, ISBN 0.935018.56.5, (1993) 114-121

- [5] Canadian Standards Association, "Engineering Design in Wood (Limit States Design)", National Standard of Canada CAN/CSA-086.1-M89.CSA, Rexdale Ont., Canada (1989)
- [6] Ehlbeck, J., Gortlacher, R. and Werner, H., "Determination of Perpendicular-to-grain Tensile Stresses in Joints with Dowel-type-fasteners", CIB-W18A Meeting, Berlin Germany, paper 22-7-2 (1989)
- [7] Rahman, M.U., Chiang, Y.J. and Rowlands, R.E., "Stress and Failure Analysis of Double-bolted Joints in Douglas-fir and Sitka Spruce", *Wood and Fiber Science*, **23** (4) (1991) 567-589
- [8] Bouchair, A., Modélisation non Linéaire du Comportement Local des Assemblages Bois, Thèse de l'Université Blaise Pascal, Clermont-Ferrand (1993)
- [9] Whitney, J.M. and Nuismer, R.J., *Journal of Composite Materials*, **8** (1974) 253-265
- [10] Larsen, H.J. and Gustafsson, P.J., "Design of End-notched Beams", CIB-W18A Meeting, Berlin Germany, paper 22-10-1 (1989)
- [11] Valentin, G. and Adjanohoun, G., "Applicability of Classical Isotropic Fracture Mechanics Specimens to Wood Crack Propagation Studies", *Materials and Structures*, **25** (1992) 3-13
- [12] Valentin, G., Boström, L., Gustafsson, P.J., Ranta-Maunus, A. and Gowda, S., "Application of Fracture Mechanics to Timber Structures", RILEM state-of-art Report, Technical Research Centre of Finland, Espoo Finland, Research Notes 1262, ISBN 951.38.3891.1 (1991)
- [13] Boström, L., "The fictitious crack model - A fracture mechanics approach applied on wood", International Conference on Timber Engineering, Seattle DC, 2, (1988) 559-565.
- [14] Bengougam, A. and Dubois, F., "Simulation de la Rupture dun Assemblage en Bois Boulonné", LMT, Mémoire de D.E.A. de l'ENS. de Cachan (1994)
- [15] Gautherin, M.T., "Critère de Contrainte Limite du Bois Massif", LMT, Thèse de l'Université Paris 6 (1980)
- [16] Johnson, J.A., "Crack Initiation in Wood Plates", *Wood Sci.*, **6** (2) (1973) 151-158

- [17] Guitard, D., "Mécanique du Matériau Bois et Composites", Cépadues-Editions, ISBN 2.85428.152.7. (1987)
- [18] CTBA, "Étude des Caractéristiques Mécaniques du Sapin et de l'Épicéa - France Entière", Rapport interne
- [19] Rathkjen, A., "Failure Criteria for Wood", Failure Criteria of Structured Media, Boehler (ed.), Balkema, Rotterdam The Netherlands, ISBN 9.06191.179.6. (1993)
- [20] Sobue, N., Scientific Report for the "Grant-in Aid Scientific research", n°62560174, Ministry of Education, Science and Culture, Japan (1989)
- [21] Griffith, A., "The Phenomena of Rupture and Flow in Solids", Philosophical Transactions of the Royal Society of London, Series A, **221** (1920) 163-198
- [22] Nallathambi, P. and Karihaloo, B.L., "Notched beam test: Mode I Fracture Toughness", Fracture Mechanics Tests for Concrete, Report of Technical Committee 89-FMT, RILEM, edited by Shah S.P. and Carpinteri A., Chapman and Hall, London, (1991) 1-86
- [23] Larsen, H.J. and Gustafsson, P.J., "The Fracture Energy of Wood in Tension Perpendicular to the Grain", CIB-W18A Meeting, Lisbon Portugal, paper 23-19-2 (1990)
- [24] Daudeville, L., Yasumura, M. and Lanvin, J.D., "Fracture of Wood in Tension Perpendicular to the Grain: Numerical Simulation by Damage Mechanics", CIB-W18A Meeting, Copenhagen Denmark, (to appear in 1995)

RÉSUMÉ

Analyse de la rupture d'un assemblage en bois boulonné

Le travail présenté concerne la modélisation et la simulation de la rupture d'un assemblage par tige métallique d'éléments de bois lamellé collé lorsque le phénomène majeur de dégradation est celui de la fissuration parallèlement au fil. Nous nous sommes pour l'instant limités à une sollicitation perpendiculaire au fibres, l'amorçage et la propagation de la fissuration, en mode I dans ce cas, sont étudiés. L'analyse de la propagation d'une fissure est effectuée au moyen de la Mécanique Linéaire Élastique de la Rupture (MLER). L'amorçage de la fissuration est prédit par l'utilisation d'un critère simplifié prenant en compte la contrainte moyenne sur une distance supposée caractéristique du matériau.

Les simulations numériques sont comparées à des résultats d'expérimentations pour divers diamètres de tiges et paramètres structuraux. Nous comparons les valeurs simulées et expérimentales des forces d'amorçage de la fissuration ainsi que des forces maximales que l'assemblage peut supporter. Afin de vérifier que la valeur identifiée du taux de restitution d'énergie critique G_c est caractéristique du matériau, une campagne d'essais de fissuration parallèlement au fil du bois par flexion trois points a également été menée sur des éprouvettes de type CIB.

Cette étude montre que la MLER peut être appliquée pour la simulation de la rupture d'un assemblage et peut être un outil pour l'amélioration des codes de dimensionnement des assemblages lorsque le phénomène majeur de dégradation du bois est celui de la fissuration parallèlement au fil.

FIGURES AND TABLES

Fig. 1: Glued laminated specimen under perpendicular to the grain loading

Fig. 2: Specimen and CD gages

Table 1: Specimens

Table 2: Initiation and ultimate experimental loads (kN)

Table 3: Initiation and ultimate computed loads (kN)

Fig. 3: B2-4 load-displacement curve ($d=20$ mm ; $e_1=7d$; $e_2=4d$)

Fig. 4: C1-1 load-displacement curve ($d=12$ mm ; $e_1=7d$; $e_2=4d$)

Fig. 5: B2-4 load-strain curve ($d=20$ mm ; $e_1=7d$; $e_2=4d$)

Fig. 6: Finite element modeling

Fig. 7: Average stress criterion

Fig. 8: Initiation load with respect to the bolt diameter ($e_1=7d$; $e_2=4d$)

Fig. 9: Initiation load with respect to the edge-distance e_2/d ($d=12$ mm ; $e_1=7d$)

Fig. 10: $Y = G \propto \left(\frac{b}{p}\right)^2$ with respect to the crack length A/d ($e_1=7d$)

Fig. 11: $Y = G \propto \left(\frac{b}{p}\right)^2$ with respect to the crack length A/d ($e_1 = 25d$)

Fig. 12: Force with respect to the crack length for the C1-1 specimen ($d=12$ mm ; $e_1=7d$; $e_2=4d$)

Fig. 13: Ultimate load with respect to the edge-distance ($e_1 = 7d$; $e_1 = 25d$)

Fig. 14: Ultimate load with respect to the bolt diameter ($e_1 = 7d$; $e_2 = 4d$)

Fig. 15: Force-displacement curve of a fracture test

Fig. 16: Bending test for the determination of the fracture energy in tension perpendicular to grain

Fig. 1

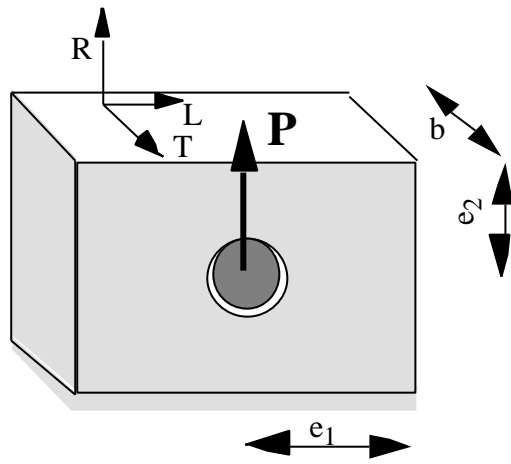


Fig. 2

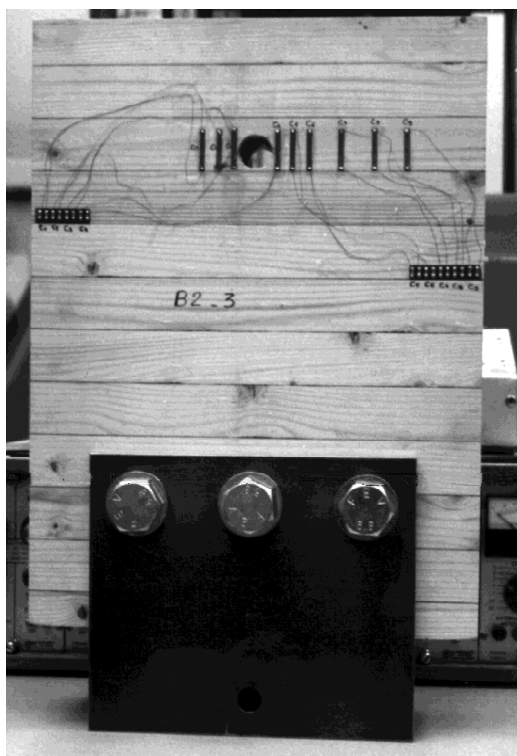


Table 1

ref.	d(mm)	b/d	e₁/d	e₂/d
A1	12	3	7	4
A2	12	3	7	8
A3	12	3	7	12
B1	16	3	7	4
B2	20	3	7	4
C1	12	3	25	4
C2	12	3	25	8
C3	12	3	25	12

Table 2

specimen	initiation load	ultimate load
A1-1	4.50	4.95
A1-2	4.00	5.03
A1-3	4.70	5.18
A1-4	4.30	4.84
A1-5	4.60	5.22
A2-1	4.40	5.10
A2-2	*	6.09
A2-3	4.10	4.87
A2-4	*	5.22
A3-1	4.30	4.90
A3-2	4.50	5.44
A3-3	4.80	5.07
B1-1	8.00	10.5
B1-2	6.40	8.49
B1-3	7.28	10.38
B2-1	10.00	14.7
B2-2	*	14.6
B2-3	9.70	11.99
B2-4	10.50	13.8
C1-1	5.20	6.27
C1-2	6.10	6.19
C2-1	*	7.35
C2-2	4.60	8.72

* means an impossibility for the authors to propose an initiation load

Table 3

specimen	initiation load	ultimate load
A1	4.34	5.58
A2	4.40	5.86
A3	4.41	5.87
B1	6.85	8.6
B2	10.05	12
C1	4.57	6.5
C2	4.85	8.7
C3	4.92	10

Fig. 3

Fig. 4

Fig. 5

Fig. 6

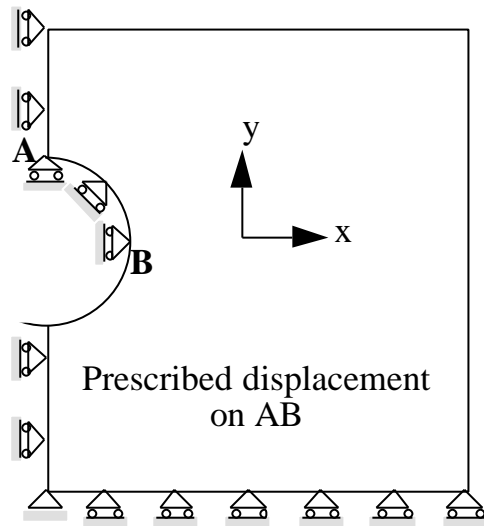


Fig. 7

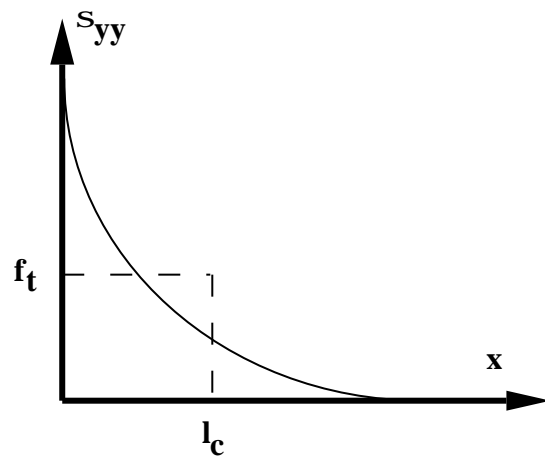


Fig. 8

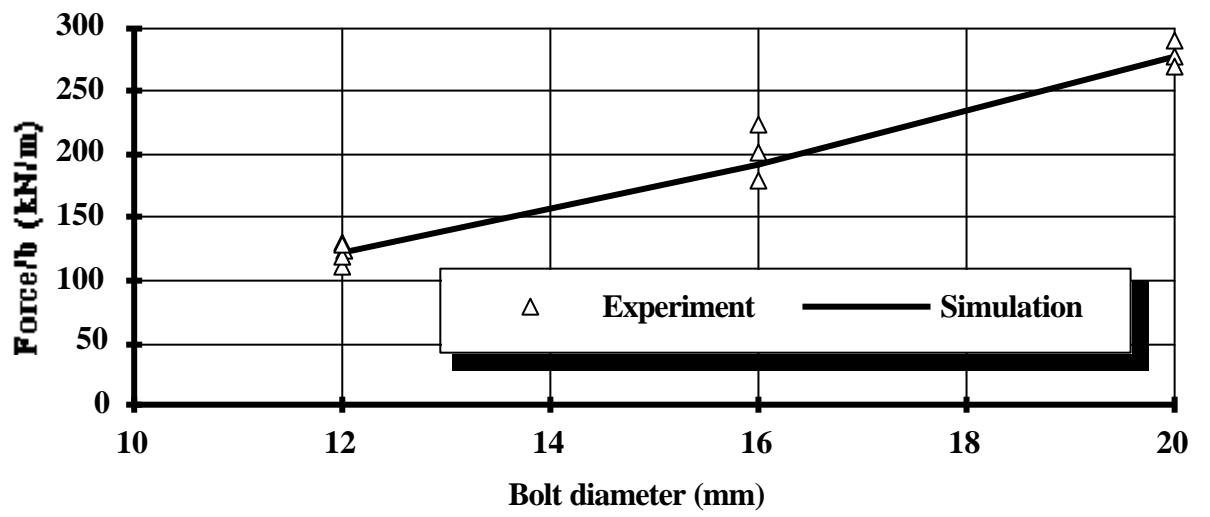


Fig. 9

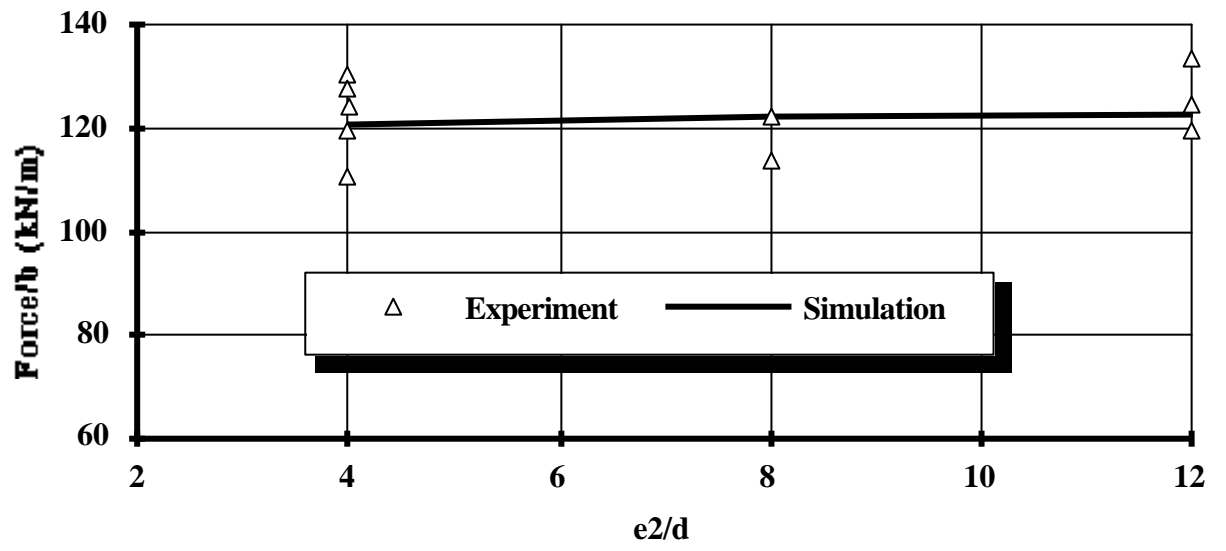


Fig. 10

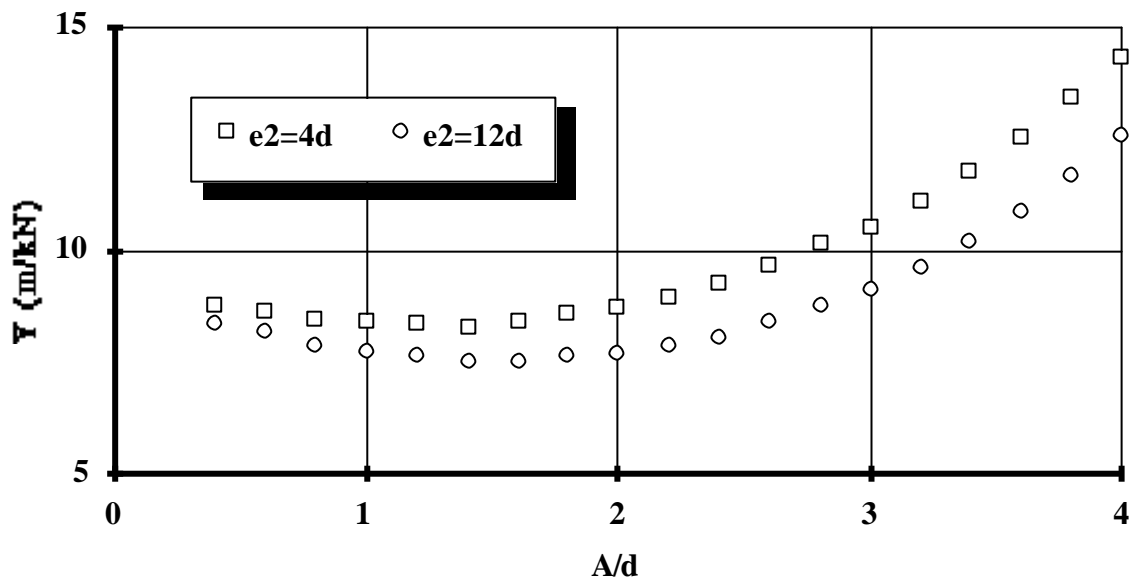


Fig. 11

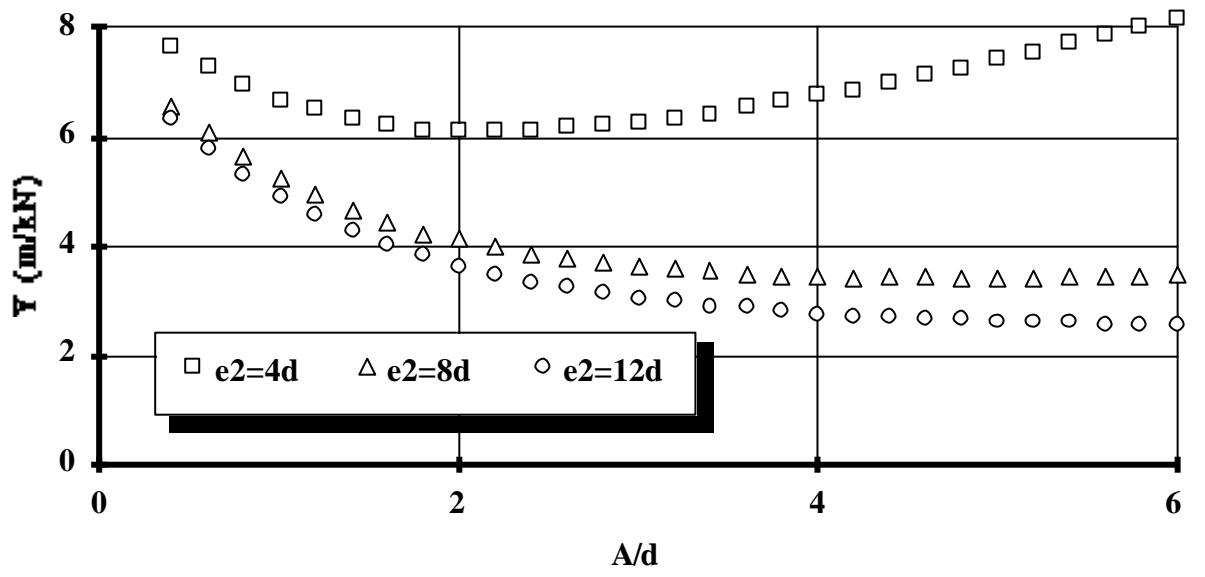


Fig. 12

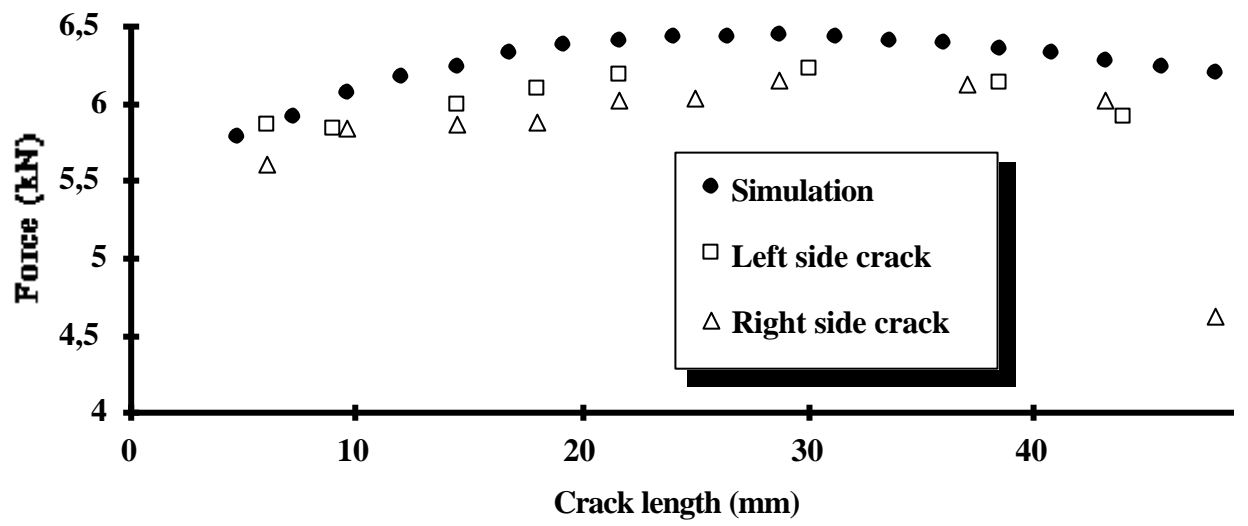


Fig. 13

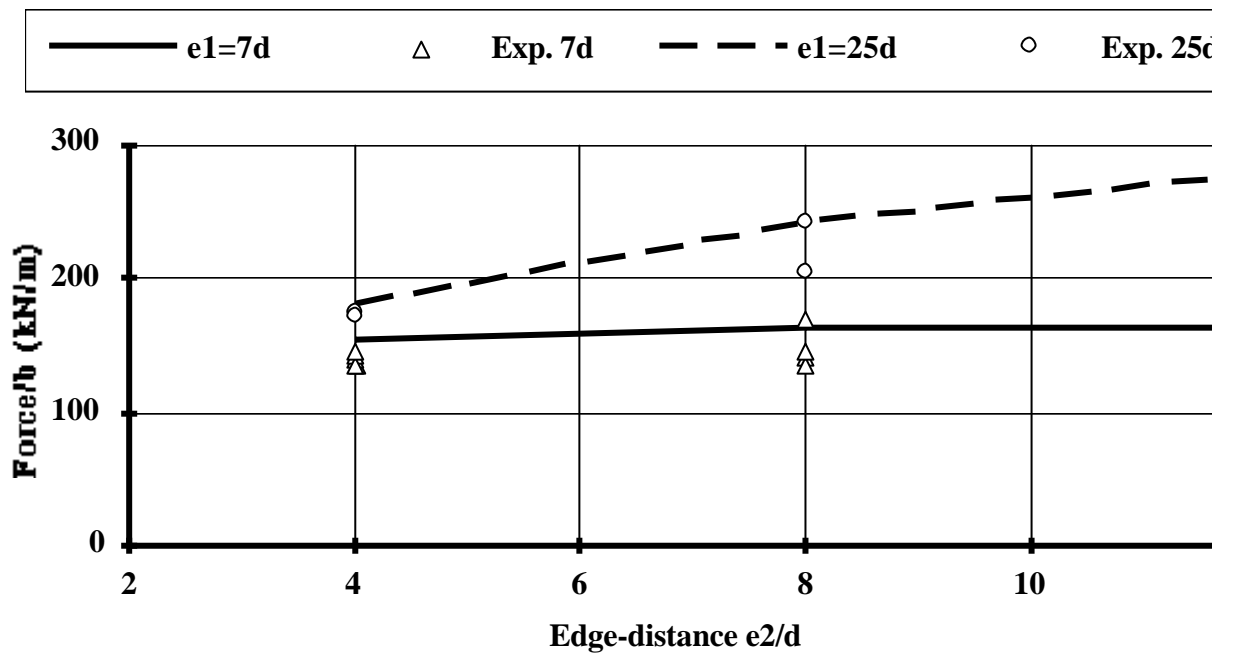


Fig. 14

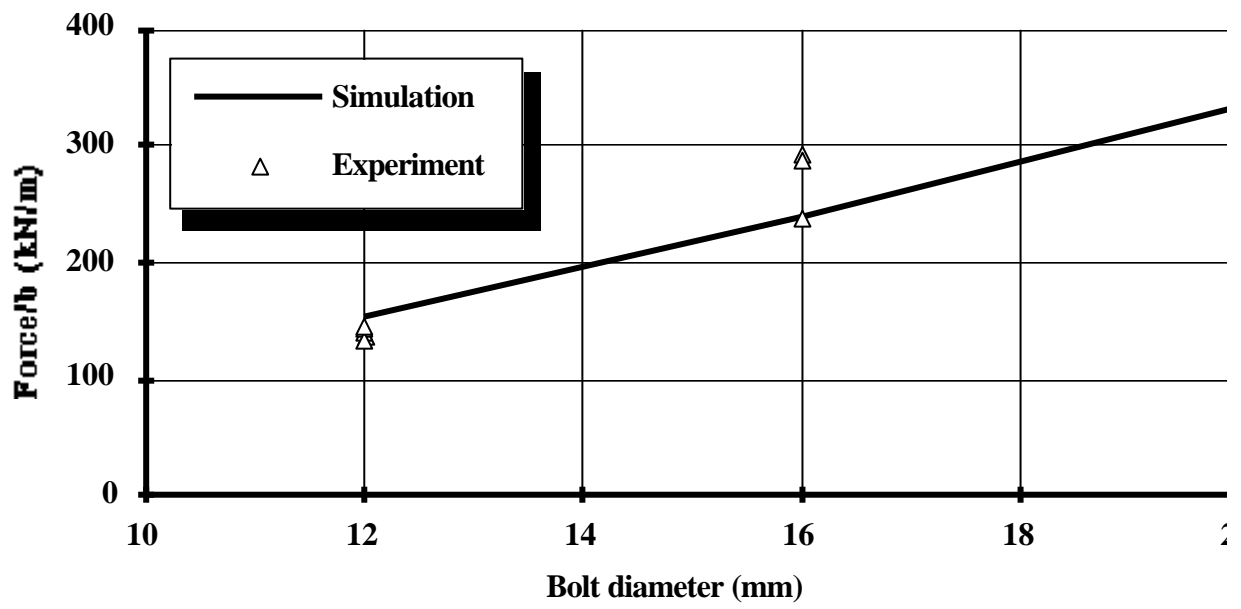


Fig. 15

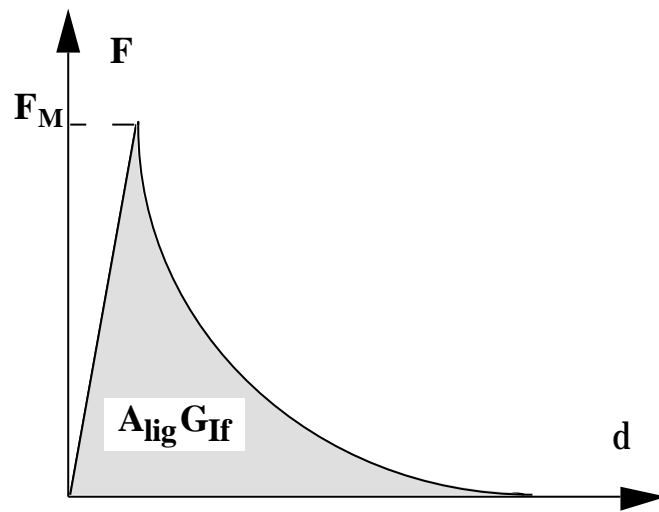


Fig. 16

